International Journal of Pharmaceutics 395 (2010) 104–113

Contents lists available at ScienceDirect

International Journal of Pharmaceutics

journal homepage: www.elsevier.com/locate/ijpharm

Coating uniformity assessment for colored immediate release tablets using multivariate image analysis

Salvador García-Muñoz*, Daniel S. Gierer

Pharmaceutical Development, Pfizer Global R & D, 445 Eastern Point Road, Groton, CT 06340, USA

ARTICLE INFO

Article history:
Received 15 February 2010
Received in revised form 3 May 2010
Accepted 15 May 2010
Available online 24 May 2010

Keywords:
Film coating
Multivariate image analysis
Principal Components Analysis
PCA
PLS

ABSTRACT

Multivariate image analysis (MIA) was applied to quantitatively assess film-coated tablets providing a cost-effective tool to replace visual inspection. MIA was used to determine the cosmetic end-point of the film-coating step and to calculate the coating level and distribution across tablets. The technique relies on simple digital images of the tablets and multivariate latent variable methods such as Principal Components Analysis (PCA) and Projection to Latent Structures (PLS). This application has precedence in the food industry and is a useful tool in *Quality by Design* by providing quantitative ranges on coating targets. The technique is illustrated using two sizes of tablets coated at two different scales. As expected, the coating distribution across tablets for the larger scale is broader, and the total amount of coating material is proportional to the surface area of the tablet. The technique is illustrated with off-line images taken with a Single-Lens Reflex digital camera, and with in-line images taken with a webcam installed inside the coater. For the latter case a novel adaptive PCA modeling approach is proposed to handle the real-time images and translate them into indexes that determine the cosmetic end-point of the film-coating step.

1. Introduction

Film coating is a common processing step in the manufacture of tablets, considered for either functional or cosmetic purposes. The practice of film coating typically relies on the gravimetric determination of the percent weight increase of the tablet as it acquires coating material during the coating run. The target for this percent weight increase is determined at the development stage; and for immediate release products – where the coating is non-functional – this determination is mostly based on the visual inspection of color uniformity of the tablets. This color uniformity is well known to be dependent on multiple driving forces acting on the operation, primarily on the mixing regime of the tablets inside the coater as the coating pan rotates. The practice of film coating would benefit from a cost-effective and robust method to determine tablet coating levels and coating uniformity that is not biased by human appreciation, especially since tablet color uniformity is commonly considered an important quality attribute of the final product.

Although well understood from a thermodynamic perspective (am Ende and Berchielli, 2005), film coating is a process that still offers challenges with respect to predicting the coating uniformity of the tablets at the end of the run (Turton, 2008). Researchers have addressed this problem from multiple angles ranging from regression analysis, non-dimensional numbers (Mueller and Kleinebudde, 2007) and Monte Carlo simulations (Pandey et al., 2006; Joglekar et al., 2008), to the use of advanced computing techniques such as Discrete Element Modeling (Fichana et al., 2009). These modeling approaches inevitably need a quantitative way to determine the coating distribution across tablets in order to estimate model parameters, or to validate simulation results. Otherwise the validity of the model is left to human opinion.

This work presents the application of Multivariate image analysis (MIA) to quantitatively determine coating levels and coating distribution of tablets from simple digital images. This technique provides both the quantitative metrics needed to validate predictive models, and a cost-effective method to aid the development and practice of the film-coating operation.

2. Multivariate image analysis (MIA)

Color assessment studies on film-coated tablets are reported in the literature for various applications, for example, to measure the change in color of a tablet due to degradation (Nyqvist and Nicklasson, 1982; Berberich et al., 2002) or as a surrogate quality control test for other properties such as tablet hardness (Siddiqui and Nazzal, 2007). These color studies are traditionally carried out using a tristimulus colorimeter and the "CIE (L^*a^*b) Formula" to quantitatively measure the color differences of the tablets (CIE

* Corresponding author. Tel.: +1 860 715 05 78.
E-mail address: salvador.garcia-munoz@pfizer.com (S. García-Muñoz).

0378-5173/$ – see front matter © 2010 Elsevier B.V. All rights reserved.
doi:10.1016/j.ijpharm.2010.05.026

Colorimetry Committee, 1974). Originally developed as a tool for the textile industry, the "CIE 1976 (L^*a^*b) Formula" was chosen by its ability to predict the human perception of color (McLaren, 1976). Color differences measured with the CIE 1976 (L^*a^*b) formula reported a coefficient of correlation of 0.7 in a study comparing these quantities with the corresponding psychological scale values of color differences as judged by human perception. This method does not produce an image but produces three values (each number equivalent to a stimulant as measured by the colorimeter) that are ultimately summarized in the scalar ΔE (McLaren, 1976) that overall quantifies the color appearance of the object analyzed.

Beyond the study of the visible color of the tablets, an area of prolific growth is that of chemical imaging. Numerous papers are found in the literature where tablets are imaged using the combination of a variety of spectroscopic instruments and a microscope. These analyses produce images of $n \times m \times ch$ (where n and m are the pixels per side of the image and ch is the number of channels measured by that particular instrument). A recent review by Gendrin et al. (2008) provides a detailed summary of some reported work in this area, specifically towards pharmaceutical applications. These applications are mostly oriented towards studying the distribution of the drug in the tablet and do not rely on color, but on non-visible spectra. The analysis of these images usually involves the use of multivariate methods to extract chemically relevant data from the spectra (Gendrin et al., 2008).

Multivariate image analysis (MIA) is a combination of the two afore mentioned approaches, it relies on color differences as detected by a conventional digital camera and stored in the form of a Red-Green-Blue image of $n \times m \times 3$ (the image has three channels, the Red the Green and the Blue) and uses multivariate methods to extract the features of the image that are relevant to the product property of interest. The main advantages of MIA over colorimetric methods and chemical imaging are the simplicity and the cost, since digital cameras are quite common and inexpensive. The obvious disadvantage is the fact that MIA depends on color differences, which limits the method from applications related to the chemical composition of the tablet where the color of the active ingredient is the same as the color of the excipients. These applications are very well handled by chemical imaging technology. A thorough literature review and short tutorial on MIA is provided in Appendix A.

Herein MIA was applied to determine the end-point of cosmetic tablet film coating and to quantify the coating distribution across tablets. As will be discussed, MIA has proven its usefulness in replacing human appreciation, thus providing an unbiased determination of the necessary amount of coat to overcome mixing inefficiencies in the pan-coater (typical of large scale coating). The technique is illustrated using off-line images and on-line images. The presented off-line MIA exercise uses the covariance method by Yu and MacGregor (2003). The on-line MIA exercise presented in this work uses a modeling approach originally proposed to monitor batch processes (adaptive Principal Components Analysis). In the proposed application, the diagnostics from the adaptive PCA mode are used to determine the cosmetic end-point of the film-coating step in real time.

3. Materials, processing and imaging conditions

The application of MIA is illustrated with two examples: the first one uses images that are taken off-line with a Single-Lens Reflex (SLR) Fujifilm S91000 digital camera (F2.8, 1/200 s shutter speed, ISO200, and 9 megapixel image resolution). The second example uses images that are taken on-line with a Logitech QuickCam® Pro 9000 camera installed inside the coater during the run (auto settings, manual white balance, and 3 megapixel image resolution).

Table 1
Relevant characteristics of the considered tablets in this study.

	Total weight (mg)	Weight RSD	Shape	Surface area (mm^2)
Tablet 1	100	<3%	Oval	127.4
Tablet 2	100	<3%	Triangular	127.6
Tablet 3	175	<3%	Triangular	184.5
Tablet 4	400	<3%	Standard round convex	267.15

The shape, total weight and surface areas of the considered tablets are listed in Table 1. Formulation details are not provided since this information is not relevant to the studies presented in this work. Off-line images were acquired using a *Mini-Repro* copy stand (Gruppo Manfrotto, Italy) using 4 fluorescent lights (14 W, 60 Hz, 200 mA); on-line images were illuminated with the light that the Vector LDCS coater is equipped with.

The off-line case study was done to quantitatively compare the coating end-point and coating uniformity between a small tablet (Tablet 1 and Tablet 2, which are considered equivalent due to their surface area) and a large tablet (Tablet 3) when coated in a small scale coater (Vector HCT-60) and a large scale coater (Glatt GC 1000). Hence four different lots (or runs) were analyzed: small tablet at small and large scale, and large tablet at small and large scale. The on-line case study was done to explore the performance of an adaptive modeling approach to determine cosmetic end-point in real-time, this second case study focuses more on the proposed mathematics and is illustrated with one tablet size (Tablet 4) coated at one scale (Vector LDCS-5). The coating material used in all cases was Red Opadry® II, sprayed in a 15% solid aqueous suspension. Processing conditions for all scales (Table 2) were selected by the formulator and are considered representative of a typical film-coating run.

4. Methods

4.1. Principal component analysis

Given a matrix **X** of n rows and m columns, a Principal Component Analysis (PCA) model with A principal components can be fitted to the data set to simplify its dimensions from m to A variables. PCA eases the analysis of the system where the data was originated and has been widely applied for process improvement (MacGregor et al., 2005) and chemometrics (Brown et al., 2009) among other fields of science. The PCA model (Eq. (1)) provides a factorization of an approximation of the original data (**X**) given by the product of matrices **T** (scores matrix of $n \times A$) and **P** (loadings matrix of $m \times A$) with an associated residual (**Ex**). In the original data, each observation or sample was represented with m variables; after PCA each observation (or sample) will be represented by A variables instead of m (given by the columns of **T**). This approximation is possible since PCA will factorize a significant amount of the variability in **X** in a much smaller number of A new variables, referred to as principal components.

The relationship between **X** and **T** is given by Eq. (2) and is a simple linear relationship of **X** with the coefficients in the **P** matrix.

Table 2
Key processing conditions for the film-coating step.

Coater	Vector HCT-60	Glatt GC 1000	Vector LDCS-5
Batch size	14 kg	56.5 kg	1.75 kg
Spray guns	2	3	1
Spray rate	80 gr/min	170 gr/min	25 gr/min
Nozzle type	Vector AT	Schlick GCSD 2.1	Schlick ABC
Inlet air temp.	68 °C	65 °C	60 °C
Outlet air temp.	40 °C	47 °**C**	48 °C

Table 3
Sampling points for each run in the off-line example.

Tablet	Coater	Sampling protocol
Tablet 2	Vector HCT-60	Samples taken at 0.40%, 1.0%, 1.4%, 1.7%, 2.0%, 2.4%, 2.8%, 3.1%, 4.5%, 4.8% and 5.1% increased weight from tablet core weight.
Tablet 3	Vector HCT-60	Samples taken at 0.1%, 0.25%, 0.4%, 0.8%, 1.0%, 1.4%, 1.9%, 2.1%, 2.5%, 2.8%, 3.2%, 3.6%, 3.9% and 4.3% increased weight from tablet core weight.
Tablet 1	Glatt GCA 1000	Samples taken at 0.25%, 0.5%, 0.75%, 1.0%, 1.5%, 2.0%, 3.0% and 4.0% increased weight from tablet core weight.
Tablet 3	Glatt GCA 1000	Samples taken at 0.25%, 0.5%, 0.75%, 1.0%, 1.5%, 2.0%, 3.0% and 4.0% increased weight from tablet core weight.

While the original m variables could exhibit some degree of correlation, the new variables (referred to as scores and given by $\mathbf{T}$) are orthogonal and generally with better signal to noise ratio than the original data. The importance of each principal component is ranked in terms of the fraction of the total variability in the data that is captured by that component (the first principal component will capture more variability than the second, than the third, etc). It is common practice to refer to the A column vectors of the $\mathbf{T}$ matrix as $\mathbf{t_1}, \mathbf{t_2}, \ldots, \mathbf{t_A}$.

$$\boldsymbol{X} = \boldsymbol{T}\boldsymbol{P}^{\mathrm{T}} + \boldsymbol{E}_X \quad (1)$$

$$\boldsymbol{T} = \boldsymbol{X}\boldsymbol{P} \quad (2)$$

The model can also be applied to additional data from the system if the model (in this case the loadings $\mathbf{P}$) is believed to hold for that new data set. This is done using Eq. (2) replacing $\mathbf{X}$ with the new data set (e.g. $\mathbf{T_{new}} = \mathbf{X_{new}}\mathbf{P}$).

More details and properties of PCA are available elsewhere (Wold et al., 1987; Edward Jackson, 1991).

4.2. Method used in the off-line case study

Tablets were taken from the pan-coater at different points throughout the film-coating step. The percent increase in weight due to coating was measured using an analytical balance for each group of tablets (three repeats of 100 tablets). Each group is further subdivided into smaller portions (of random amounts) to be imaged. Tablets were pictured in a random order against a black background; each sub-portion is imaged multiple times. The random ordering of the tablets allows for sufficient exposure of the band and both faces of the tablets. The collected images are deemed representative of the batch at each sampling point. Each sampling point is referred to by the measured percent weight increase measured from the tablets at that time (Table 3). Camera settings and distance to object were kept constant for all the images taken.

MIA was then applied to the collection of images corresponding to each run separately. The method is described as it was applied individually to each run. More details on the method can be found in the paper by Yu and MacGregor (2003), as their method was applied consistent to their description with the addition of a minor step (step 2) to remove the background from the image.

1. A composite image is built using a randomly chosen image from each sampling point. This composite image is used to fit a PCA model that is later applied to all images of the lot in order to calculate the scores ($\mathbf{t_1} - \mathbf{t_2}$) for each image. These scores are used to create a 2D histogram-scatter score plot per image. The addition of coat (and the resulting of the change in color) is clearly evident in the score plots for varying amounts of coating material in the tablets (Fig. 1) as the higher density regions shift from left to right and slightly to the bottom.
2. An image of the background is taken under the same focus as if tablets were present in the image (*Auto Focus* is locked with tablets in the image frame, tablets are removed and the picture is taken). This image of pure background is then evaluated using the PCA model to estimate its corresponding scores ($\mathbf{Tb} = [\mathbf{tb_1}\ \mathbf{tb_2}]$). These scores ($\mathbf{Tb}$) are then used to establish a mask in the score space by fitting the matrix of scores for the background ($\mathbf{Tb}$) to secondary PCA model with two principal components (referred to as PCAb for clarity). The 99% joint confidence interval for the scores in the PCAb model is used to build an elliptical mask in the histogram-scatter score space. This mask is used to identify all the pixels corresponding to the background, independently of their position in the original image. The use of the secondary PCA model (PCAb) is a simple way to rotate the coordinates of $\mathbf{tb_1}$ and $\mathbf{tb_2}$ and determine the mask corresponding to the space mapped by the background pixels. Alternative geometric manipulations will give the same result. Fig. 2 illustrates this background removal step: the bottom image is the histogram-scatter plot with all pixels corresponding to the background removed (hence elliptical black shape in the right side of this image), and the top image in Fig. 2 is the original image with all the identified background pixels displayed in pure white.
3. The 2D histogram-scatter plots for each image (with the background pixels removed) are manipulated according to the covariance method (Yu and MacGregor, 2003) to finally identify a covariance mask that will maximize the feature extraction for the property of interest, which in this case is the percent weight

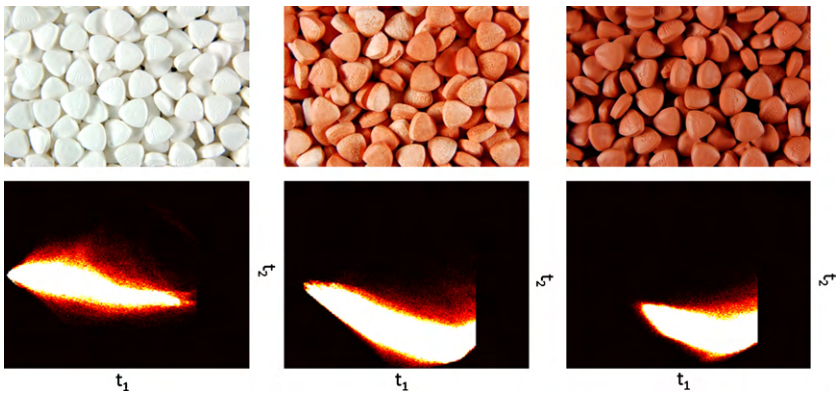

Fig. 1. 2D score histogram-scatters for images of tablets with varying amounts of coat.

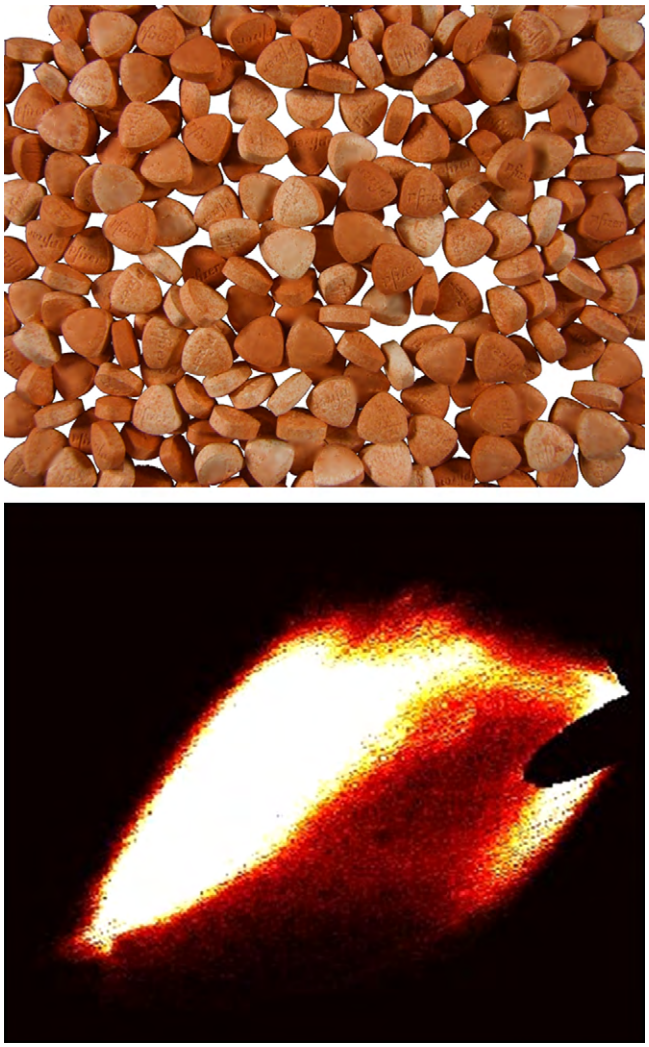

Fig. 2. Background removal example, bottom plot: histogram-scatter plot with background pixels removed, top plot: original image with all background pixels shown in pure white.

increase due to coating. The covariance mask is applied to the 2D histogram-scatter plots of all the background-free images, creating a feature vector for each image which is normalized by the total number of pixels in the image. This normalization makes the method robust to varying number of tablets in the image or the varying amounts of background removed.

4. At this point there is one feature vector per image, and multiple images per pull point (hence multiple feature vectors per pull point). The collection of all feature vectors is collected into a matrix (**F**). The **F** matrix has as many observations (rows) as images taken, and as many columns as bins in the covariance mask (Yu and MacGregor, 2003). A PCA model with one principal component is fitted to matrix the **F** (referred to as PCA_F for clarity). The scores of the PCA_F model are used to determine the cosmetic end-point since the scores will plateau when the average color in the image is no longer changing.
5. A Projection to Latent Structures (PLS) model is fitted using the average feature vector per pull point as a regressor and its measured weight increase due to coating as a response. This regression model is used later to determine the distribution of coating across each image.
6. Each available image is subdivided into small images of approximately the same area as one tablet. A feature vector is calculated per sub-image as described before. The PLS model is then used to predict the amount of coating in each sub-image by using its corresponding feature vector. The collection of predicted coating contents for the sub-images of all the images for a pull point are used to determine a distribution which is normalized to a total frequency count of 100 and represents the distribution of coating (by % weight increase) observed in the imaged, normalized to 100 tablets.

The obtained distributions are used as a quantitative guide in establishing the acceptable range of levels of coating (normally one sided range) in support of a *design space* (Food and Drug Administration, 2006).

4.3. Method used in the on-line case study

The on-line application of MIA is well precedented (Yu et al., 2003; Liu et al., 2004; Tessier et al., 2008), and in all cases involve the use of a time-invariant model applied to new samples. This application of MIA is well suited for stationary settings (for either continuous or batch processes) where the physical environment is not disturbed (lights, angles, distances and orientations are kept in place) and hence the model parameters can be assumed to be constant. This is not the case for a lot-based pharmaceutical manufacturing environment where machinery is constantly being disassembled, implying a drastic disturbance to the physical setting where the images are taken. Under these circumstances, a new modeling effort (or re-calibration step) would be necessary each time the system is re-assembled.

This particular scenario where one would need to build and use a new model for every batch was recognized by Rannar et al. (1998) and addressed with the use of an adaptive PCA modeling approach. In this approach a PCA model is fitted with information initially available and then updated as new samples become available from the process. The method is quite straight-forward and uses one tuning parameter commonly referred to as the *forgetting factor* (d_k) in adaptive control literature, or the *weighting factor* in an exponentially weighted moving average (EWMA) model.

This parameter (d_k) determines the relative importance of the new sample with respect to the past information already contained in the PCA model. In such an adaptive approach, a d_k value of zero will imply that the new data is irrelevant and the model (and all its diagnostics) will never change; a value of d_k much higher than one implies that the data available from the past is irrelevant and the model (and its diagnostics) will depend almost solely on the data available in the new sample. Lower values of d_k result in slow model adaptation while high values of d_k result in fast model adaptation.

As the PCA model adapts to new samples, so will its diagnostics (such as the scores). A measure of model stability can easily be established by a running standard deviation on the time-varying values of the model diagnostics, such as the mean value for the scores ($\boldsymbol{\mu}_T$ a vector where each element corresponds to the mean value of each of the A columns of **T**). When the model is no longer changing (new data is no different from past data), the running standard deviation of the diagnostics will be at its lowest value, which is determined by the sensitivity of the data acquisition device (the camera in this case).

This method was applied as follows to the case where images were taken during the film-coating operation, and the appearance of the product is expected to transition from initial to a final color appearance.

(1) Determine and fix the forgetting factor d_k, and the window size for the running standard deviations (ws). This last parameter (ws) will determine how many past values of $\boldsymbol{\mu}_T$ are to be kept

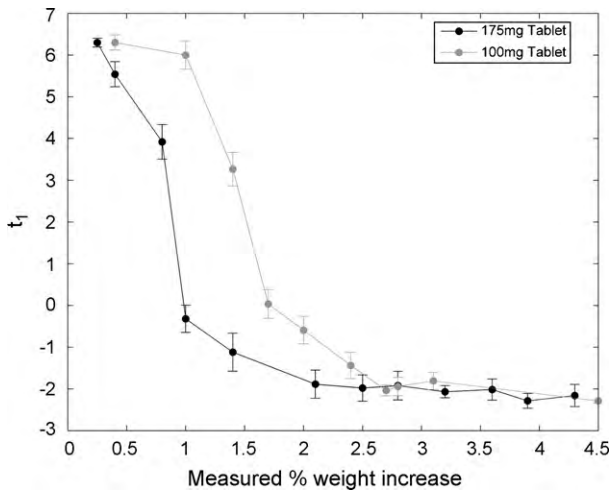

Fig. 3. Score plots for the 1st principal component of feature vectors corresponding to the images taken of two tablet sizes coated in a small scale coater.

in order to calculate the running standard deviation of the mean values for the scores.

(2) An initial image is taken and a PCA model is fitted with the image data rearranged as an $(n \times m) \times 3$ matrix (where n and m are the pixels per side of the image). The initial mean values for the scores ($\boldsymbol{\mu}_T$) are estimated from the scores of this model ($\mathbf{T}$). *As images become available (steps 3–5).*

(3) Update the PCA model according to the process defined in the literature (Rannar et al., 1998) using the data from the new image and the d_k value. Estimate new mean values for the scores ($\boldsymbol{\mu}_T$).

(4) Compute a running standard deviation using the last *ws* values of $\boldsymbol{\mu}_T$. Only *ws* values of $\boldsymbol{\mu}_T$ need to be kept, always discarding the oldest value.

(5) Assess the values of the running standard deviations to determine if the model is stable and hence the images are no longer different in their color appearance.

As will be shown, there is always residual variability in the running standard deviation, in this case given by the changing image where tablets are always in different presentation to the camera. Improved optics and illumination might reduce this variation. Although inexpensive optics were used for this work, it was observed that the technique performed well in determining the end-point for cosmetic appearance, as later verified by visual inspection.

5. Results

5.1. Off-line case study

As mentioned before, the objective of this part of the study is to compare the evolution of the distribution of coating between two tablet sizes when coated at two scales. For length considerations, only selected plots are shown to illustrate the nature of the results obtained with MIA.

As discussed in the methods section, once the background is removed and the feature vectors are extracted from the images, a PCA model is fitted to the **F** matrix of feature vectors. The scores from these PCA models are the first result of physical importance since these are a quantitative indication of the change of color appearance of the tablets.

The rate at which the appearance of the tablets changes during the film-coating operation is illustrated in Fig. 3. This figure shows the change in the average value of the first principal component ($\mathbf{t_1}$) for two tablet sizes (Tablet 2 and Tablet 3, see Table 1) coated in the HCT-60 coater. It is only the first component that needs focus since the major change in tablet appearance (from bare tablet cores to fully coated tablets) is dominant. The error bars in Fig. 3 correspond to the 95% confidence intervals for the mean value, and these are obtained with the mean $\mathbf{t_1}$ values for multiple images taken of the product at each pull point. This plot is particularly useful to determine the cosmetic end-point for the operation; this is the point in which the average tablet is fully coated. It is important to point out that Fig. 3 represents an unsupervised diagnostic, since this plot is the result of the natural evolution of the image signature.

Table 4
Correlation coefficients for the different PLS models used to determine coating distributions.

Tablet	Coater	R^2
Tablet 2	HCT-60	99%
Tablet 1	Glatt GC 1000	97%
Tablet 3	HCT-60	94%
Tablet 3	Glatt GC 1000	97%

In order to determine the coating distribution across an image, a regression model needs to be calibrated between the image feature vector, and the measured increase in tablet weight. The quality of the obtained regressions is shown in Fig. 4, and the correlation coefficients for each model are listed in Table 4. The error bars in Fig. 4 correspond to the 95% confidence interval in the prediction which is mainly driven by the image-to-image differences at each pull point.

Each of the regression models was then used to determine the coating distribution across one image (as discussed in the Methods section). The histograms of the multiple values of the coating level across all of the sub-images for a pull point are the basis to calculate the final coating distribution for each pull point. The distribution of coat across tablets, as it changes throughout the coating run (i.e. the evolution of coating distribution) for Tablet 3 is illustrated in Fig. 5. The evolution of the coating distribution at the large scale is shown in the upper plot of Fig. 5, and the one at the small scale coater is shown in the bottom plot. The arrows in each illustrate the difference between the average coating level and the lower tail of the distribution.

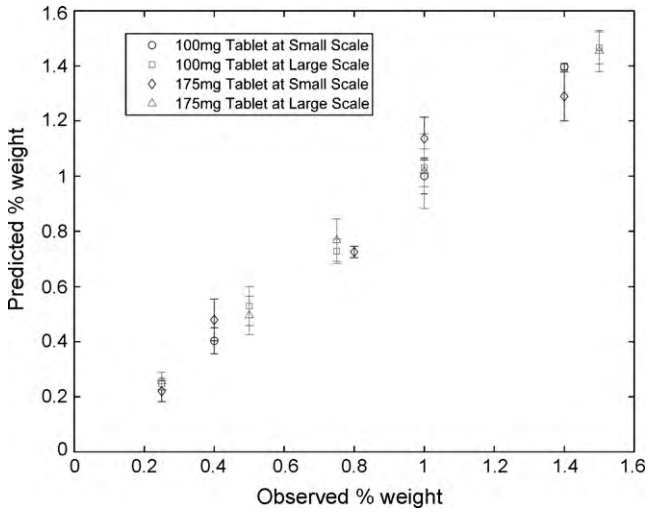

Fig. 4. Observed versus predicted percent increase due to coating using a regression model based on image features.

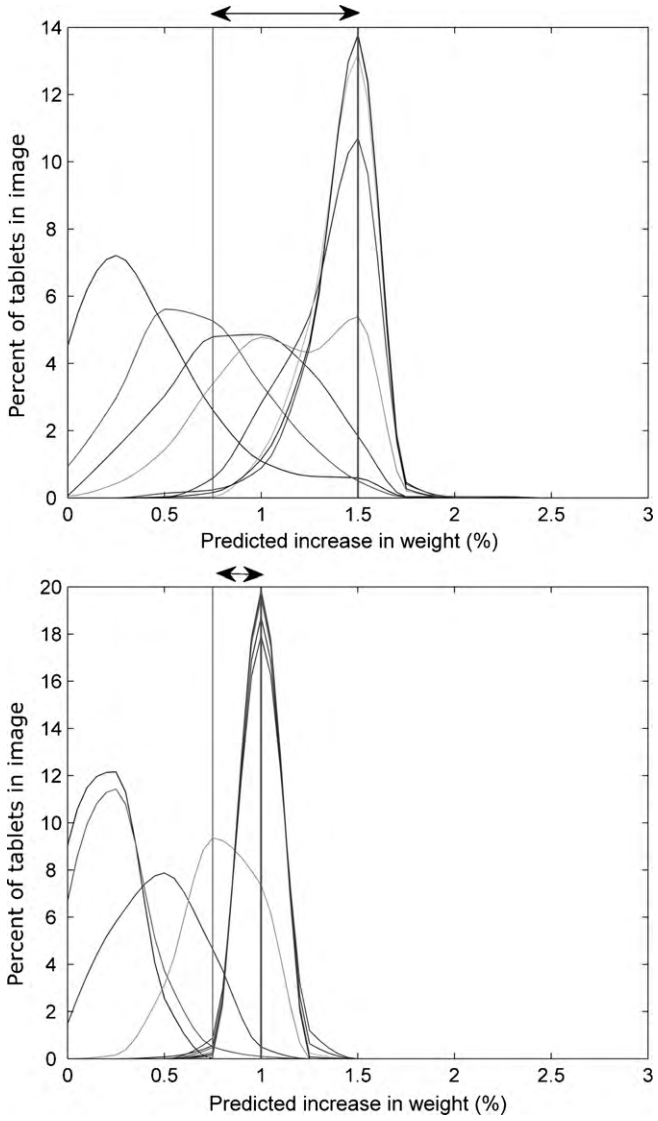

Fig. 5. Evolution of coating distribution for a 175 mg triangular tablet coated in a HCT-60 coater (bottom) and a Glatt GC1000 coater (top). Arrows illustrate the span between the mode of the coating distribution and lower tail.

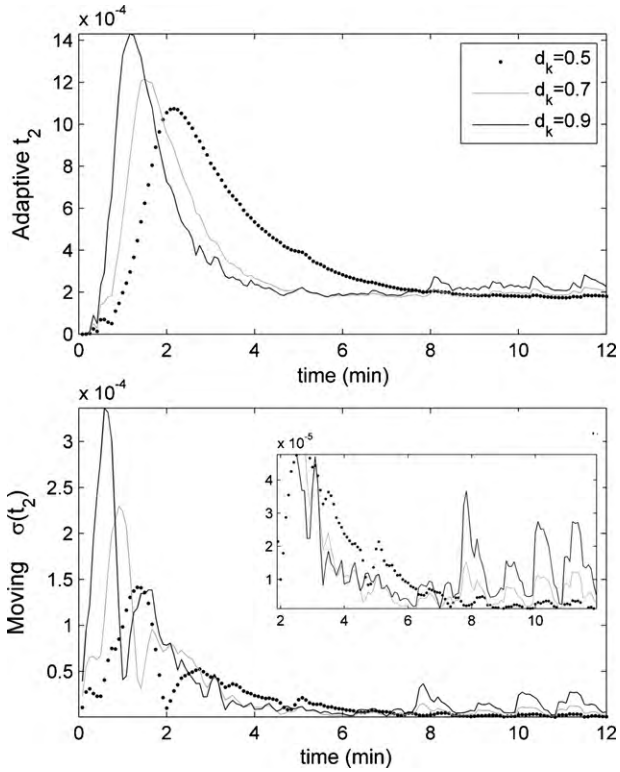

Fig. 6. top: adaptive $\mathbf{t_2}$ value for real-time MIA calculated form on-line images in the LDCS-5 coater, bottom: running standard deviation of the adaptive $\mathbf{t_2}$ value shown in the upper plot.

5.2. On-line case study

This case study involves the coating of Tablet 4 in an LDCS Vector coater (see Tables 1 and 2). Images were taken every 5 s. The analysis of the images is performed using three values for the forgetting factor (d_k) and for all cases a window of 5 samples to calculate the running standard deviation. Results obtained for the second principal component as they change with time are illustrated in Fig. 6, where the upper plot corresponds to the adaptive value of $\mathbf{t_2}$, and the bottom plot corresponds to the values of the moving standard deviation for $\mathbf{t_2}$. Similar plots are available for $\mathbf{t_1}$ and are not shown for length considerations.

6. Discussion

The comparison done with MIA on tablets that were imaged off-line yielded results that corresponded to prior knowledge and experience. Due to the larger collective surface area, small tablets reach coating uniformity at a slower rate than larger tablets (with a smaller collective surface area) as it was observed in the change of the natural image signature (illustrated in Fig. 3). In this plot it can be seen that the color signature of the larger tablet changed at an earlier point than the smaller one. This behavior was observed at both small and large scales, the color of large tablets stabilizes earlier than smaller one.

The end-point for cosmetic coating was determined by analyzing the mode and the spread of the estimated coating distribution as it changes throughout the film-coating step (Fig. 5). The mode of these distributions will evolve from zero coating to a certain predicted weight increase that tends to stabilize (bold vertical gray lines in Fig. 5). This is the point where the appearance of the tablet is no longer changing, and additional amounts of coat will not result in a change in color. This point is referred to as the average cosmetic end-point.

The spread of the distributions needs to be considered as well. To ensure that all tablets will have the necessary amount of coat to be on or above the cosmetic end-point; an additional amount of coat is considered. This amount depends on the span of the distribution towards the low end and is equal to the difference between the mode of the distribution and the lower end of the tail (illustrated by arrows in Fig. 5). This additional amount will be smaller for a coater with a more efficient mixing regime, and will increase as the mixing becomes more inefficient.

Although this decrease in mixing efficiency is mainly a factor of scale, there are other factors to consider such as the baffle arrangement, the rotational speed of the pan, the coating suspension spray rate and the shape of the tablet. MIA could potentially be used to study the effect of these factors on the coating of the product given a proper experimental design geared towards decoupling the effect of each of these factors. The final amounts of coat to apply for the tablets studied are listed in Table 5. Notice that although the average weight gain does not change dramatically with scale; the amount of coat needed to overcome mixing inefficiencies does change significantly from one scale to the other.

Table 5
Cosmetic end-points as determined by MIA.

Summary of MIA Results for IR film-coated tablets		HCT-60 Triangular 100 mg Tablet	Glatt GC1000 Oval 100 mg Tablet	HCT-60 Triangular 175 mg Tablet	Glatt GC1000 Triangular 175 mg Tablet
Average weight gain from MIA	Function of tablet surface area and Opadry composition	2.50%	2.60%	1%	1.5%
Weight gain additional threshold due to table mixing	Function of coating process parameters, scale and mixing regime	0.70%	1.20%	0.17%	0.70%
Total target weight gain (%)		3.20%	3.80%	1.17%	2.20%
Pan load		14 kg	56.5 kg	14 kg	56.5 kg

Two parallel measurements are in fact required in the application of MIA one being the images taken from the tablets and the other being the measured weight increase of the coated tablets. The images of the tablets will change as coating is applied until they reach the cosmetic end-point; MIA will pick up the variability in color appearance among the tablets in the image irrespectively of their weight. The color features of the images will then be tied to a given measure of weight increase; and this measured weight increase could potentially be subject to variability from one tablet to another. The fact that the model behind MIA is fitting the mean color signature with the mean weight increase in a population of tablets will largely hinder the effect of tablet core weight variability on the results of the method. Once the model behind MIA has been established and validated, then the weight measurement can be left to the end of the run (after the end-point is detected by MIA) for verification purposes only.

With respect to the results obtained for the on-line exercise: the upper plot in Fig. 6 represents the change in the color signature as the film-coating process evolves (as captured by the second principal component), the bottom plot is simply a running standard deviation of the diagnostic shown in upper plot. The cosmetic end-point in this case will be determined when the value of the upper plot stops to change (which in term will correspond to a value close to zero in the running standard deviation). There will be two pairs of plots since two principal components are usually enough to well model these matrices. The behavior of these plots will strongly depend on the chosen values for d_k and the window size for the standard deviation; as with all other model-based adaptive techniques, this is a known limitation of the method. Nevertheless, once a good choice of d_k and the window size are identified, these can be used for subsequent batches.

The expected behavior of an adaptive technique was observed in the obtained results: low values of d_k lead to slow adaptation of the model diagnostics which results in a longer time for the running standard deviation to settle. A d_k value of 0.5 was observed to plateau at ~7 min. Values of 0.7 and 0.9 result in similar plateau times of ~4.5 min. Using low values of d_k increases the sensitivity to changes in the image that can be seen in Fig. 6 as upward oscillations at 8, 10 and 11 min which are the times when the operator took tablet samples and the shadow of the thief was shown in the image. When compared with visual inspection, a d_k value of 0.7 was thought to be a good balance between sensitivity and stability.

7. Conclusions

Multivariate image analysis (MIA) is a useful tool in supporting the development of the film-coating *design space* used in *Quality by Design* (QbD) regulatory filings (Food and Drug Administration, 2006). This technique utilizes digital images of the tablets and multivariate latent methods to provide a reproducible, non-biased assessment of film coat tablet coverage. Using film coat weight gain as the in-process quality control mechanism, MIA can be applied to identify edges of failure for film coat coverage (cosmetic end-point) to support the establishment of the proven acceptable range (PAR) values.

A method formerly proposed to be used in batch analysis is now applied for real-time MIA to determine the cosmetic end-point as the coating progresses. A forgetting factor (d_k) of 0.7 was identified as a good choice for the system analyzed in this work. The authors believe this value should be assessed for each different manufacturing scale. Overall, real-time MIA is shown to be feasible and provides a valuable tool for situations where the operation is under tight containment restrictions.

The results of applying MIA as shown in this work were ultimately verified by visual inspection. This should not represent a limitation of the method but a natural way to verify that mathematical-based decisions match the perception of the human eye; this is after all the way current standards (CIE) were verified at the time of their development.

Finally, since the application of MIA to RGB images will exploit color differences, it is expected that this method will be limited when the color of the tablet core is very close to that of the coating material or when the coating material lacks color as in the case of clear coats that can be applied for elegance.

Acknowledgements

The authors want to thank Daniel Blackwood, Neil Turnbull, Alfred Berchielli, Mary am Ende and Angela Hausberger for their valuable comments and suggestions in completing this work and improving the manuscript. We also thank Bruce Green, Angela Kong, Anja Guntermann, Mark Polizzi, Michael Bourland and Christoph Wabel for their help in producing and collecting samples for this work.

Appendix A. Literature review and short tutorial on multivariate image analysis

The foundations of MIA were established by Geladi and his collaborators (Geladi et al., 1989, 1992; Esbensen and Geladi, 1989; Geladi and Esbensen, 1989; Geladi, 1992a, 1992b, 1995, 1996) originally focusing on the use of MIA for classification problems. This early work proposes the idea of rearranging the 3-dimensional ($n \times m \times 3$) matrix from an RGB digital image into a 2-dimensional matrix of $n \times m$ rows and 3 columns. This matrix is then decomposed using Principal Components Analysis (PCA) to generate two score vectors (referred to as $\mathbf{t_1}$ and $\mathbf{t_2}$). In the original image, each pixel was associated with a triplet of scalars (corresponding to the intensities of red, green and blue); after performing the PCA model

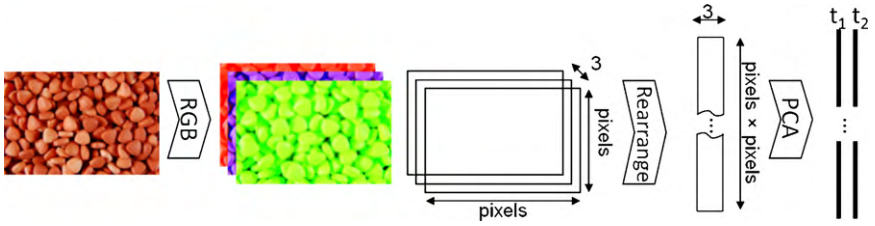

Fig. A1. Basic roadmap to multivariate image analysis.

each pixel is now represented by two scalars (corresponding to its $\mathbf{t_1}$ and $\mathbf{t_2}$ values see Fig. A1). The pixels from the original image are then placed into a score histogram-scatter of their corresponding $\mathbf{t_1}$ and $\mathbf{t_2}$ values. In this plot, pixels with similar intensities and ratios of red, green and blue will cluster together. Geometrical shapes can then be identified in the $\mathbf{t_1t_2}$ space to delineate regions that define the borders of a cluster. These shapes are referred to as *masks*. Hence, by focusing on groups of pixels that project inside a given mask, one could identify regions in the original image that exhibited similar color characteristics.

These concepts are illustrated with a simple image of two tablets. The original image (Fig. A2, top left) is decomposed by PCA. The PCA scores ($\mathbf{t_1}$ and $\mathbf{t_2}$) for all the pixels in the original image are then plotted in a two dimensional (2D) histogram-scatter (Fig. A3). Fig. A3 shows the location of the pixels in the score space and also illustrates the density of pixels in the score space by the intensity of the white color in the scatter (whiter color means more pixels project in that position of the score plot). This score histogram-scatter clearly shows five clusters. Each of these clusters corresponds to pixels with similar features in the original image irrespectively of where the pixel is located in the image. In this example, the five clusters in the score space correspond to the faces and bands of each of the tablets, and the background (everything in the image that is not a tablet). An example of a mask to isolate pixels corresponding to the band of the pink tablet is shown in blue. By selecting the pixels in each of the clusters, it is possible to accurately identify these features in the original image (Fig. A2). Fig. A2 illustrates how pixels can be separated according to their corresponding cluster in the score histogram-scatter (Fig. A3) and how this clustering correctly separates different features of the original image. The identification of these masks has been and continues to be a topic of research as will be discussed below.

MIA was taken into the process systems engineering context and proposed as a tool for industrial process monitoring and control by

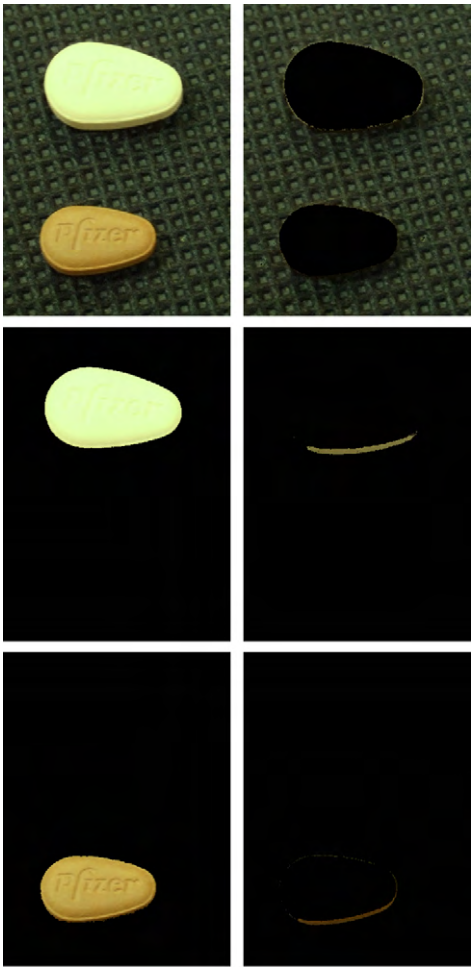

Fig. A2. Example of image segmentation using MIA. Top left: original image, top right: image background, middle left: pink tablet face, middle left: pink tablet band; bottom right: red tablet face, bottom left: red tablet band.

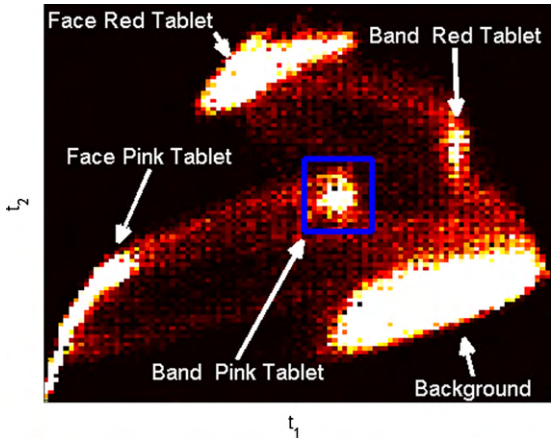

Fig. A3. Two dimensional score histogram-scatter plot built with example image (top left in Fig. 2).

Bharati and MacGregor (1998). Their work suggests that images could potentially be taken and efficiently analyzed in real time to make decisions affecting the quality of the end product. The main concept introduced by their work was that a change in the appearance of a product (as captured by digital images) could be identified by MIA as a movement of pixels in the score space (see Fig. 1 of main text). Process monitoring diagnostics can be developed, based for example on the fraction of pixels in a certain region of the score space.

The ideas established by Bharati and MacGregor were further developed by Yu and MacGregor (2003) by using the features extracted by MIA to predict a property of interest in the product. Their work proposes several methods to identify alternative masks in the score space in order to maximize the extraction of image features related to the properties of interest from the product. The covariance method (Yu and MacGregor, 2003) was later applied to the monitoring and control of the seasoning content of snack foods (Yu et al., 2003).

The techniques and methods established by Bharati, Yu and MacGregor have been extensively applied to other fields. In the pulp and paper industry, MIA was applied for automatic lumber classification (Bharati et al., 2003; Nilsson and Edlund, 2005). Lumber classification was the motivational example for the application of Support Vector Machines (SVM) to automate the identification of masks in the score space for defect detection (Liu et al., 2005b).

MIA was applied to monitor flames from industrial boilers to predict the levels of combustion gases and energy output from the flame. MIA was ideally suited for these applications since the analysis does not depend on the special arrangement of the pixels in the picture (flames are not stationary in the picture frame) (Yu and MacGregor, 2004; Szatvanyi et al., 2006).

Other areas of reported applications of MIA are the consumer goods industry (Antonelli et al., 2004; Chevallier et al., 2007; Borin et al., 2007) and the metal-metallurgic industry (Liu et al., 2005a; Tessier et al., 2008; Graham et al., 2009). In some applications MIA was coupled with texture analysis techniques to study bubbles, ceramics, fruits and semiconductors (Liu et al., 2005a; Prats-Montalban and Ferrer, 2007; Facco et al., 2009). More recently MIA was applied to analyze images taken during a crystallization process to characterize the evolution of the process (Sarkar et al., 2009); and in dermatology to predict levels of hyper-pigmentation severity in human skin replacing the visual assessment of a dermatologist (Prats-Montalban et al., 2009).

References

am Ende, M.T., Berchielli, A., 2005. A thermodynamic model for organic and aqueous tablet film coating. Pharm. Dev. Technol. 10, 47–58.

Antonelli, A., Cocchi, M., Fava, P., Foca, G., Franchini, G.C., Manzini, D., Ulrici, A., 2004. Automated evaluation of food colour by means of multivariate image analysis coupled to a wavelet-based classification algorithm. Anal. Chim. Acta 515, 3–13.

Berberich, J., Dee, K.-H., Hayauchi, Y., Portner, C., 2002. Pharmaceutical applications of vibrational chemical imaging and chemometrics: a review. Int. J. Pharm. 234, 55–66.

Bharati, M.H., MacGregor, J.F., 1998. Multivariate image analysis for real-time process monitoring and control. Ind. Eng. Chem. Res. 37, 4715–4724.

Bharati, M.H., MacGregor, J.F., Tropper, W., 2003. Softwood lumber grading through on-line multivariate image analysis techniques. Ind. Eng. Chem. Res. 42, 5345–5353.

Borin, A., Ferrúo, M., Mello, C., Cordi, L., Pataca, L., Durín, N., Poppi, R., 2007. Quantification of Lactobacillus in fermented milk by multivariate image analysis with least-squares support-vector machines. Anal. Bioanal. Chem. 387, 1105–1112.

Brown, S.D., Tauler, R., Walczak, B., 2009. Comprehensive Chemometrics. Elsevier.

Chevallier, S., Bertrand, D., Kohler, A., Courcoux, P., 2007. Application of PLS-DA in multivariate image analysis. J. Chemom. 20, 221–229.

CIE Colorimetry Committee, 1974. Working program on color differences. J. Opt. Soc. Am. 64, 896–899.

Edward Jackson, J., 1991. A User's Guide to Principal Components, 1st ed. Wiley-Interscience.

Esbensen, K., Geladi, P., 1989. Strategy of multivariate image analysis (MIA). Chemom. Intell. Lab. Syst. 7, 67–86.

Facco, P., Bezzo, F., Barolo, M., Mukherjee, R., Romagnoli, J.A., 2009. Monitoring roughness and edge shape on semiconductors through multiresolution and multivariate image analysis. AICHE J. 55, 1147–1160.

Fichana, D., Marchut, A.J., Ohlsson, P.H., Chang, S.Y., Lyngberg, O., Dougherty, J., Kiang, S., Stamato, H., Chaudhuri, B., Muzzio, F., 2009. Experimental and model-based approaches to studying mixing in coating pans. Pharm. Dev. Technol. 14, 173–184.

Food and Drug Administration, 2006. ICH Q8 Pharmaceutical Development. Pharmaceutical CGMPs.

Geladi, P., Isaksson, H., Lindqvist, L., Wold, S., Esbensen, K., 1989. Principal component analysis of multivariate images. Chemom. Intell. Lab. Syst. 5, 209–220.

Geladi, P., 1992a. Image analysis in chemistry. II. Multivariate image analysis. Trends Anal. Chem. 11, 121–130.

Geladi, P., 1992b. Some special topics in multivariate image analysis. Chemom. Intell. Lab. Syst. 14, 375–390.

Geladi, P., 1995. Sampling and local models for multivariate image analysis. Mikrochim. Acta 120, 211–230.

Geladi, P., 1996. Multivariate Image Analysis in Chemistry and Related Areas: Chemometric Image Analysis. Wiley, Chichester, UK.

Geladi, P., Bengtsson, E., Esbensen, K., Grahn, H., 1992. Image analysis in chemistry. I. Properties of images. Trends Anal. Chem. 11, 41–53.

Geladi, P., Esbensen, K., 1989. Can image analysis provide information useful in chemistry? J. Chemom. 3, 419–429.

Gendrin, C., Roggo, Y., Collet, C., 2008. Pharmaceutical applications of vibrational chemical imaging and chemometrics: a review. J. Pharm. Biomed. Anal. 48, 533–553.

Graham, K.J., Krishnapisharody, K., Irons, G.A., MacGregor, J.F., 2009. Ladle eye area measurement using multivariate image analysis. Can. Metall. Quart. 46, 397.

Joglekar, A., Joshi, N., Song, Y., Ergun, J., 2008. Mathematical model to predict coat weight variability in a pan coating process. Pharm. Dev. Technol. 12, 297–306.

Liu, J., MacGregor, J.F., Duchesne, C., Bartolacci, G., 2005a. Flotation froth monitoring using multiresolutional multivariate image analysis. Miner. Eng. 18, 65–76.

Liu, J.J., Bharati, M.H., Dunn, K.G., MacGregor, J.F., 2005b. Automatic masking in multivariate image analysis using support vector machines. Chemom. Intell. Lab. Syst. 79, 42–54.

Liu, J.J., MacGregor, J.F., Duchesne, C., Bartolacci, G., 2004. Flotation froth monitoring using multi-resolutional multivariate image analysis. Miner. Eng. 18, 65–76.

MacGregor, J.F., Yu, H., Garcia-Munoz, S., Flores-Cerrillo, J., 2005. Data-based latent variable methods for process analysis monitoring and control. Comput. Chem. Eng. 29, 1217–1223.

McLaren, K., 1976. The development of the CIE 1976 ($L \times a \times b$) uniform colour space and colour-difference formula. J. Soc. Dyers Colourists 92, 338–341.

Mueller, R., Kleinebudde, P., 2007. Prediction of tablet velocity in pan coaters for scale-up. Powder Technol. 173, 51–58.

Nilsson, D., Edlund, U., 2005. Pine and spruce roundwood species classification using multivariate image analysis on bark. Holzforschung 59, 689–695.

Nyqvist, H., Nicklasson, M., 1982. Studies on the physical properties of tablets and excipients. V. Film coating for protection of a light-sensitive tablet formulation. Acta Pharm. Suec. 19, 223–228.

Pandey, P., Katakdaunde, M., Turton, R., 2006. Modeling weight variability in a pan coating process using Monte Carlo simulations. AAPS PharmSciTech 7, E2–E11.

Prats-Montalban, J.M., Ferrer, A., 2007. Integration of colour and textural information in multivariate image analysis: defect detection and classification issues. J. Chemom. 21, 10–23.

Prats-Montalban, J.M., Ferrer, A., Bro, R., Hancewicz, T., 2009. Prediction of skin quality properties by different Multivariate Image Analysis methodologies. Chemom. Intell. Lab. Syst. 96, 6–13.

Rannar, S., MacGregor, J.F., Wold, S., 1998. Adaptive batch monitoring using hierarchical PCA. Chemom. Intell. Lab. Syst. 41, 73–81.
Sarkar, D., Doan, X.T., Ying, Z., Srinivasan, R., 2009. In situ particle size estimation for crystallization processes by multivariate image analysis. Chem. Eng. Sci. 64, 9–19.
Siddiqui, A., Nazzal, S., 2007. Measurement of surface color as an expedient QC method for the detection of deviations in tablet hardness. Int. J. Pharm. 341, 173–180.
Szatvanyi, G., Duchesne, C., Bartolacci, G., 2006. Multivariate image analysis of flames for product quality and combustion control in rotary kilns. Ind. Eng. Chem. Res. 45, 4706–4715.
Tessier, J., Duchesne, C., Gauthier, C., Dufour, G., 2008. Estimation of alumina content of anode cover materials using multivariate image analysis techniques. Chem. Eng. Sci. 63, 1370–1380.
Turton, R., 2008. Challenges in the modeling and prediction of coating of pharmaceutical dosage forms. Powder Technol. 181, 186–194.
Wold, S., Esbensen, K., Geladi, P., 1987. Principal components analysis. Chemom. Intell. Lab. Syst. 2, 37–52.
Yu, H., MacGregor, J.F., 2003. Multivariate image analysis and regression for prediction of coating content and distribution in the production of snack foods. Chemom. Intell. Lab. Syst. 67, 125–144.
Yu, H., MacGregor, J.F., Haarsma, G., Bourg, W., 2003. Digital imaging for online monitoring and control of industrial snack food processes. Ind. Eng. Chem. Res. 42, 3036–3044.
Yu, H., MacGregor, J.F., 2004. Monitoring flames in an industrial boiler using multivariate image analysis. AICHE J. 50, 1474–1483.